Journal of Interfaces, Thin films, and Low dimensional systems 5 (2) Winter and Spring (2022) 537-545

Simulation of hard X-ray time evolution in the stable region of plasma tokamak by using the NARX-GA hybrid neural network

Scientific research paper

Amir Alavi[1], Shervin Saadat[2*], Mohamad Reza Ghanbari[3], Seyed Enayatallah Alavi[4], Ali Kadkhodaie[5]

[1]*Department of Physics, Shoushtar Branch, Islamic Azad University, Shoushtar, Iran*

[2]*Canadian Light Source Inc., University of Saskatchewan, Saskatoon, Saskatchewan, S7N2V3, Canada*

[3]*Department of Basic Sciences, Garmsar Branch, Islamic Azad University, Garmsar, Iran*

[4]*Department of Computer Engineering, Faculty of Engineering, Shahid Chamran University of Ahvaz, Ahvaz, Iran*

[5]*Earth Sciences Department, Faculty of Natural Sciences, University of Tabriz, Tabriz, Iran*

ARTICLE INFO

Article history:
Received 24 June 2022
Revised 4 October 2022
Accepted 8 February 2023
Available online 22 April 2023

Keywords
Methodology
Hard X-ray
Runaway electrons
NARX-GA network

ABSTRACT

The time evolution of hard X-ray has been simulated using the NARX-GA hybrid neural network in the stable region of the plasma tokamak. Loop voltage and hard X-ray measured by the tokamak diagnostics tools were selected as network inputs. The NARX network has been trained using the Genetic Algorithm (GA) and the time evolution of the hard X-ray up to 500 μs (MSE = 4.13×10^{-5}) is accurately simulated. Increasing the confinement time is the particular purpose of applying tokamak to produce energy through fusion. The real-time application of this methodology brings us closer to this goal. Hard X-ray prediction can prevent plasma energy reduction. It can also reduce the severe damage caused by runaway electrons (RE) colliding with the tokamak wall. Early prediction of hard X-ray time evolution is critical in attempting to mitigate the REs potentially dangerous effects.

1 Introduction

Runaway electrons are the undesirable product of plasma tokamak, which are generated by the thermal quench phenomenon and increasing electric field [1]. The collision of the runaway electrons with the plasma particles and the tokamak wall is followed by hard X-ray radiation, according to the Bremsstrahlung phenomenon [2–7], which reduces the plasma energy. Hard X-ray radiation makes the tokamak environment dangerous because its energy can reach up to 100 KeV. In large tokamaks such as ITER, the runaway electrons current is about 10 MA [8–10], and their energy reaches about 10 MeV [11–17]. Therefore, the collision of these energetic electrons with the tokamak wall causes severe damage and melting the wall [18,19]. Thus, the control of runaway electrons has received much attention, and practical methods like magnetic perturbations [20–22],

*Corresponding author.
Email address: shervin.f.saadat@gmail.com
DOI: 10.22051/jitl.2023.40718.1073

massive gas injection [23,24], shattered pellet injection [25], and limiter biasing [26] are used to suppress them, while numerical models are designed to deal with REs [27–30].

Numerous diagnostics measure the critical plasma properties to control confinement conditions, and the data obtained from them are recorded in a time series. Loop voltage coil and hard X-ray detector are the two diagnostic devices used in tokamaks. Loop voltage can be measured through a voltage loop coil, which is applied to calculate plasma resistance, ohmic heating, and to survey the runaway electrons. The NaI scintillator detector is utilized to record vital X-ray data. This device should be used to limit energy reduction and destructive effects caused by the generation of runaway electrons. X-ray radiation provides valuable information about runaway electrons. Plasma nonlinearity and complexity cause theoretical methods not to be able to determine and predict plasma time evolution. Therefore, having an accurate tool with reliable performance that can predict the time evolution of plasma tokamak properties can be a solution in this regard. Time series can be predicted by AR, MA, ARMA, ARIMA, and SARIMA methods. For example, to predict plasma modes, the ARIMA method has been used [31]. Artificial neural networks (ANN) have received a lot of attention in various sciences due to their great accuracy in solving classification, pattern recognition, and prediction problems. Artificial neural networks can predict the complexity of plasma behavior [27], and be used in real-time in the tokamak control system. Artificial neural networks have been applied to classify the TCV tokamak plasma confinement modes [32]. To predict the plasma disruption time in DIII-D tokamak [33] and J-TEX tokamak [34], also to model fusion in JET tokamak [35], and for modelling the vertical plasma displacement in HL-2A tokamak [36], artificial neural networks have been utilized.

Artificial neural networks can make intelligent time series prediction methods. They can resolve stochastic and nonlinear problems [37]. Also, ANN can be applied in real-time to control runaway electrons and predict the time of X-ray emission caused by these electrons. The prediction of HXR behavior in the IR-T1 tokamak was performed by the NARX neural network using the Levenberg-Marquardt optimization algorithm, which was the first time that this method was introduced for use in the tokamak control system [38]. Optimization algorithms such as the Levenberg-Marquardt algorithm that operate based on gradients may fall into the trap of local minima in the optimization stages and do not reach the desired result, but the evolutionary Genetic algorithm does not face such a problem [39]. In this research we trained the NARX neural network, which is designed and built to predict time series, by using the genetic algorithm (GA) and the network accurately that predicted the time evolution of hard X-rays. This method can be used in the tokamak control system in real time and can be effective in reducing the destructive effects of the runaway electrons in the tokamak. This methodology can increase plasma confinement time and increase tokamak quality efficiency. The genetic algorithm as an optimization algorithm has found a special place in various sciences [40–48].

This article is organized as follows: Section 2 is devoted to the generation of runaway electrons. Section 3 introduces the NARX-GA hybrid neural network. Section 4 deals with how to simulate the time evolution of hard X-rays, and in the conclusion section, the results are presented.

2 Runaway electron generation

Two known factors cause the first generation of runaway electrons in tokamak plasma: increasing the electric field and thermal quench.

A toroidal electric field is required to confine the plasma. If this field increases, the electric force can overcome frictional forces, and the electrons will run away [49,50]. The electric field required for electrons to reach a critical speed is called the Dreiser field.

$$E_D = \frac{ne^3 \ln\Lambda}{4\pi \epsilon_o^2 T_e}, \quad (1)$$

where, e, n, $\ln\Lambda$, $\epsilon_\circ$, T_e, and are respectively the electron charge, electron density, Coulomb logarithm, vacuum permeability, and the electron bulk temperature

The reasons for the rapid cooling of plasma in tokamaks are different [1]. Changing the position of the plasma and its collision with the tokamak wall can lead to the influx of particles and impurities into the plasma. Radiation caused by plasma colliding with impurities as well as energy transfer to the tokamak wall leads to loss of plasma heat energy [1]. This can cause the plasma to cool rapidly (in milliseconds), which is called a thermal quench. This dramatic decrease in temperature causes a

sharp increase in plasma resistance. Plasma current is related to an electric field through Ohm's law as

$$j_{th} = \frac{E_{||}}{\rho}. \quad (2)$$

If $E_{||}$ does not change, the increase in resistance causes a rapid decrease in the plasma current. However, the inductive property of the system prevents a significant change in current at such short time scales. It causes a sharp increase in the parallel electric field to maintain the current. Plasma current quench usually occurs much longer than thermal quench. Thus, there will be a strong electric field over a significant period that leads to the generation of runaway electrons. There is another process for the generation of runaway electrons, which is the second generation mechanism. In this process, secondary runaway electrons are generated by colliding of the existing runaway electrons with thermal electrons (Avalanche mechanism) [51–53].

Collision of runaway electrons with plasma particles and tokamak wall produces hard X-rays. The hard X-rays received by the detector contain vital information about the runaway electrons. Therefore, the hard X-rays produced by the runaway electrons are used to study the time evolution of their collisions. For example, the resonant magnetic perturbation method is used to reduce the destructive effect of RE in the ASDEX tokamak, and by comparing hard X-rays with the case where resonant magnetic perturbations are not used, it can be seen that the X-ray energy is reduced [54]. The Argon injection method has been used to reduce the energy of runaway electrons in the DIII-D tokamak, and by measuring the hard X-ray after using this method, the reduction of the energy of the hard X-ray has been evident [55]. To calculate the energy of runaway electrons, hard X-rays produced by these electrons have been used in the JET tokamak [56]. The spatial distribution of runaway electrons in the DIII-D tokamak is studied by an array of HXR scintillators [38].

3 NARX-GA Hybrid Neural Network

The NARX is a dynamic network with feedback that the output is returned back as input [57]. Dynamic networks are efficient in predicting time series. The equation defined for the NARX network is as follows

$$y(t) = f(x(t-1), x(t-2), \ldots, x(t-d), y(t-1), y(t-2), \ldots, y(t-d)) \quad (3)$$

where the output value y(t) is obtained using the previous values of the output signal and the previous values of the input signal from the regression method by the network. The training of this network is supervised. To use the NARX, the network architecture and its inputs must be selected. After entering the inputs, the network randomly divides the inputs and outputs into three groups: train data, validation, and test. Train data, which is about 70% of the data, is used to train the network to determine the appropriate weights and biases. About 15% of the data, as validation data, evaluates the network training at the same time as the training process and prevents over-fitting. 15% of the data as test data. After the training process, evaluate the trained network. To optimize network performance, a quantitative criterion called performance function is used that compares network outputs with target data. To reduce the value of the performance index, various optimization algorithms are applied, such as the gradient descent algorithm, Newton algorithm, and Levenberg-Marquardt algorithm, which are based on the gradient. Such algorithms may be trapped in local minima during the optimization process. To overcome such a problem, evolutionary algorithms such as genetic algorithms can be used to train the NARX network. The genetic algorithm is inspired by the survival of a generation of more successful and graceful species. This algorithm starts the optimization by randomly generating an initial population of problem solutions in chromosome form. The chromosomal structure generated is evaluated, and the chromosomes that are closest to the problem solutions are selected as the parent generation. Parents, by using the processes of crossover and mutation, create the next generation of chromosomes (offspring), and this process continues until optimal solutions are reached. The use of genetic algorithms as optimization algorithms in artificial neural networks in various sciences has provided very accurate results and has received much attention.

4 Results and discussion

4.1 Inputs and architecture of the networks

The NARX-GA hybrid neural network was applied to simulate the time evolution of hard X-rays using

MATLAB software. For this purpose, it is necessary to select the appropriate inputs and determine the network architecture correctly, both of which have particular importance. The data recorded by the IR-T1 tokamak diagnostics were used to select the network input, which included plasma current (IP), loop voltage (Vloop), Mirnov coil data (MP), and data recorded by the hard X-ray (HXR) detector. Each IR-T1 tokamak diagnostic records measured data every half microsecond; therefore, in the stable region of the plasma, about twenty thousand data are recorded, which is the desirable statistical population. Network inputs can be determined by the correlation between the inputs and the target data or using the trial and error method. Since the current and energy of the runaway electrons depend on the temperature, density, and loop voltage [58], Vloop could be a proper option for selecting network input. To ensure this choice, we used the MATLAB software to get the correlation value between Vloop data and HXR data, which was an excellent value of 0.94. So we selected Vloop as the network input. IP and MP data did not correlate well with HXR data and also were used by the trial and error method as network input. The best results were obtained using Vloop as input. Choosing the right network architecture plays a vital role in the quality of performance and speed of training. Table 1 shows the components used in the network architecture.

Table1. Specifications and architecture of the NARX-GA network.

Number of Layers	Number of Hidden Layer Neurons in	Hidden Layer Activation Function	Output layer Activation Function	Performance Function	Training Algorithm
2	10	Tansig	Purelin	MSE	GA

4.2 Simulation of hard X-ray time evolution

We repeatedly used the NARX-GA network to simulate the behavior of hard X-rays throughout the plasma time evolution in the stable region. We evaluate the network performance at all stages. According to the plasma current profile (Fig. 1 (a)), the stable region is seen. The tournament method was used to select the generations. In the production of the new generation, 35% of the chromosome was used for mutation and 50% for crossover, and we considered 25 iterations as the stop criterion for network training.

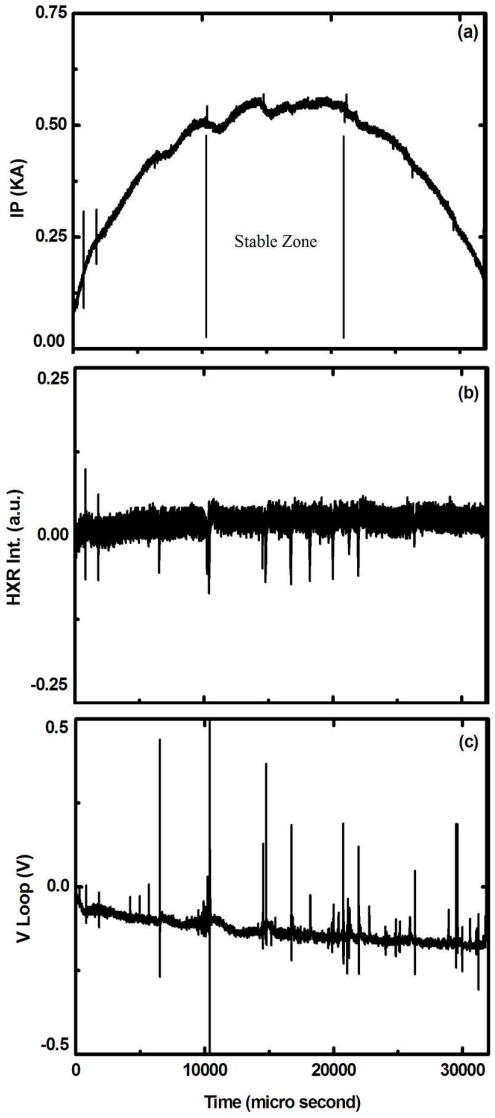

Figure 1. The time evolution of (a) Plasma current, (b) HXR intensity, and (c) Vloop.

Figures 2, 3, and 4 show the prediction of 500 and 1000 multi-steps of hard X-ray time evolution using 5000 data from Vloop and HXR inputs in the stable region. The best results are obtained with 5000 data from each input [27]. In these figures, the blue dashed line represents the actual data (target), and the solid blue line represents the trained data of the NARX-GA network. The red dashed line denotes the real data during the

forecast period (real data), and the solid red line represents the predicted value of the NARX network (predicted).

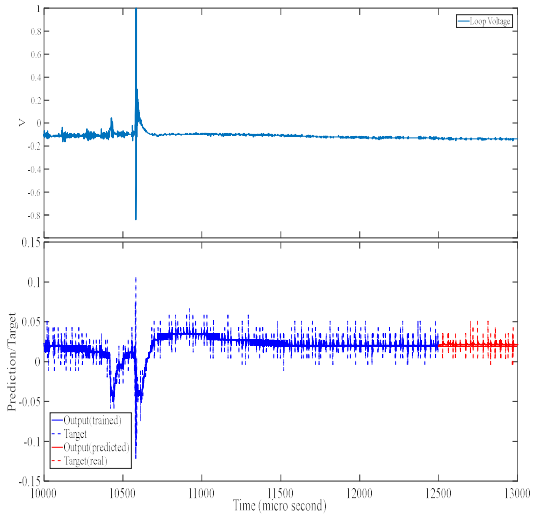

Figure 2. Top, loop voltage. Bottom, simulation of HXR time evolution in the stable region of the plasma tokamak in the range of 12500-13000 μs.

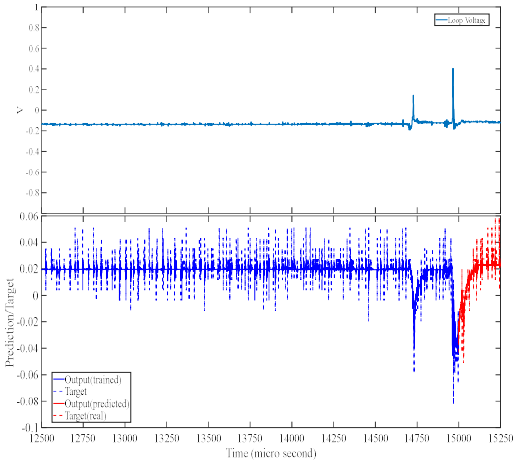

Figure 3. Top, Loop voltage. Bottom, simulation of HXR time evolution in the stable region of the plasma tokamak in the range of 15000-15250 μs.

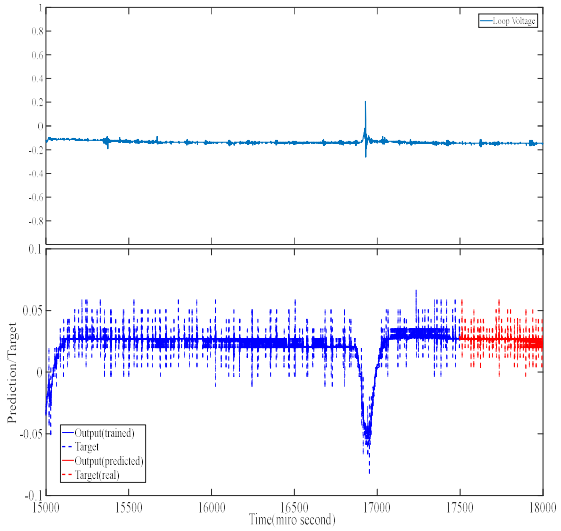

Figure 4. up: Loop voltage, down: Simulation of HXR time evolution in the stable region of the plasma tokamak in the range of 17500-18000 μs.

4 Conclusions

The NARX-GA neural network was used to simulate the time evolution of hard X-rays in the stable region of the plasma. An open loop coil is used to measure the plasma voltage, which is placed parallel to the plasma column. Any change in the plasma current causes a change in the magnetic flux passing through the loop voltage which can be seen in the time evolution of Vloop (Figs. 2-4). Based on the Bremsstrahlung phenomenon, collisions of runaway electrons with plasma components and tokamak wall produce hard X-rays, which can be seen in the time evolution of HXR (Figs. 2-4). These collisions cause a change in the magnetic flux in the voltage loop and the fluctuations in the Vloop profile show the same. From the comparison of the time evolution of HXR and Vloop, it can be clearly seen that with changes in Vloop, HXR also changes. This is a confirmation of the accuracy of the operation and the accuracy of the diagnosis used. Figures 5 to 9 show the magnifying of the 500 steps from the forecast section of Figs. 2 to 4, which show that the network has been able to accurately predict when hard X-rays will occur and when no radiation has been emitted. The network was able to predict the trend and relatively severe fluctuations of hard X-ray time evolution with high accuracy. Tables 2 to 4 show the performance results of these predictions. The excellent performance of the training data reflects the high quality

of the network training by the genetic algorithm. The performance of validation data also shows that over-fitting has not been done and is a confirmation of the excellent quality of network training. Also, the performance of the test data is a confirmation of the high quality of the trained network. All of these performances indicate that the network architecture is significantly selected and the simulation results are very reliable. These results show the great capability and accuracy of the NARX-GA network.

Table 2. The NARX-GA performance in the stable region in the range of 1000-13000 μs.

Train Data Performance	Validation Data Performance	Test Data Performance	Network Performance	Network Accuracy
5.52×10^{-5}	3.38×10^{-5}	3.33×10^{-5}	4.87×10^{-5}	High

Table 3. The NARX-GA performance in the stable region in the range of 12500-15250 μs.

Train Data Performance	Validation Data Performance	Test Data Performance	Network Performance	Network Accuracy
3.28×10^{-5}	3.43×10^{-5}	3.12×10^{-5}	3.27×10^{-5}	High

Table 4. The NARX-GA performance in the stable region in the range of 15000-18000 μs.

Train Data Performance	Validation Data Performance	Test Data Performance	Network Performance	Network Accuracy
4.07×10^{-5}	4.75×10^{-5}	4.75×10^{-5}	4.27×10^{-5}	High

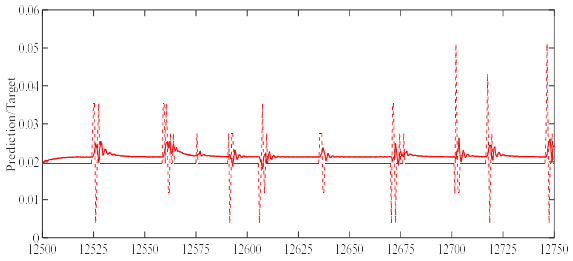

Figure 5. Magnifying of the first 500 steps of the prediction section of Fig 2.

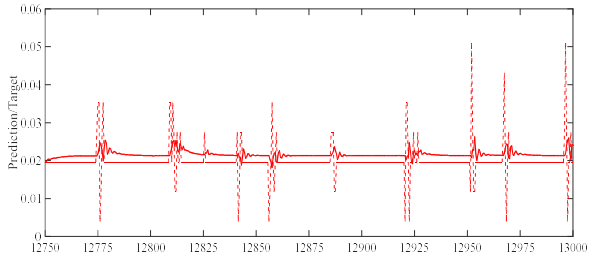

Figure 6. Magnifying of the second 500 steps of the prediction section of Fig 2.

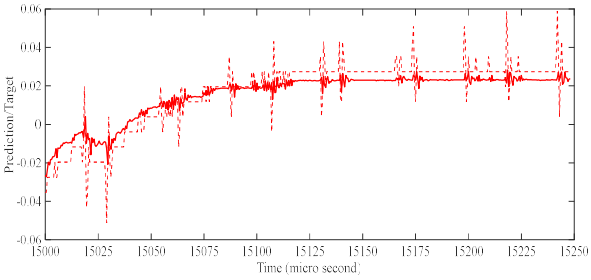

Figure 7. Magnifying of the 500 steps of the prediction section of Fig 3.

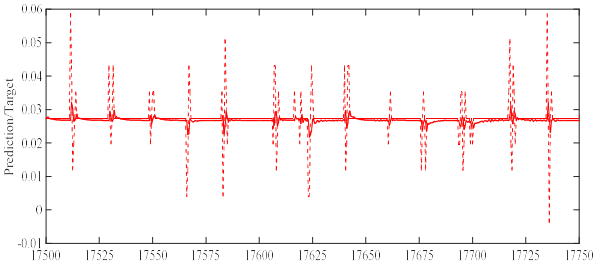

Figure 8. Magnifying of the first 500 steps of the prediction section of Fig 4.

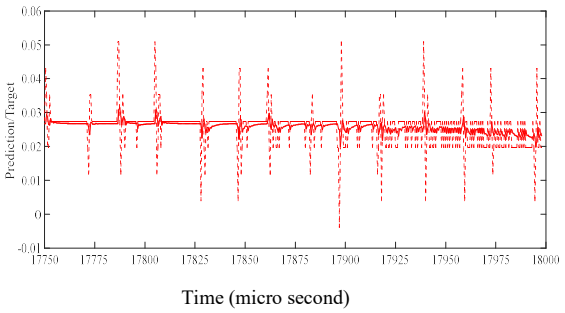

Figure 9. Magnifying of the second 500 steps of the prediction section of Fig 4.

Due to the excellent results of the NARX-GA network in simulating the time evolution of hard X-rays, it is possible to use this methodology in the tokamak control system with confidence. Radiation can be prevented by accurately predicting the time of occurrence of hard X-rays. The time evolution of hard X-ray determines the time of the collision of the runaway electrons with the plasma components or with the tokamak wall. In this paper, the time evolution of HXR is predicted. That is, the time of occurrence and energy of collisions can be predicted before their event. This method states that it is possible to predict the collision time of the runaway electrons with the plasma components and the tokamak wall in real time. Therefore, the tokamak control system can prevent a runaway electron collision just when it is predicted to occur using methods such as resonant magnetic perturbation, Argon injection, or other available methods. It can effectively reduce the damages caused by the collision of these electrons to the tokamak wall and the enormous costs.

References

[1] B. N. Breizman et al., "Physics of runaway electrons in tokamaks. "Nuclear Fusion, **59** (2019) 083001.

[2] M. Bakhtiari et al., "Role of bremsstrahlung radiation in limiting the energy of runaway electrons in tokamaks." Physical review letters, **94** (2005) 215003.

[3] R. D. Gill, "Generation and loss of runaway electrons following disruptions in JET." Nuclear Fusion, **33** (1993) 1613.

[4] R. D. Gill et al., "Direct observations of runaway electrons during disruptions in the JET tokamak." Nuclear Fusion, **40** (2000) 163.

[5] L. Novotny et al., "Runaway electron diagnostics using silicon strip detector." Journal of Instrumentation, **15** (2020) C07015.

[6] A. Dal Molin et al., "Novel compact hard x-ray spectrometer with MCps counting rate capabilities for runaway electron measurements on DIII-D." Review of Scientific Instruments, **92** (2021) 043517.

[7] A. Shevelev et al., "Study of runaway electrons with Hard X-ray spectrometry of tokamak plasmas." AIP Conference Proceedings, **1612** (2014) 125.

[8] L. G. Eriksson et al., "Current dynamics during disruptions in large tokamaks." Physical review letters, **92** (2004) 205004.

[9] S. Mirnov et al., "MHD stability, operational limits and disruptions." Nuclear Fusion, **39** (1999) 225.

[10] A. H. Boozer, "Runaway electrons and ITER." Nuclear Fusion, **57** (2017) 056018.

[11] R. D Gill et al., "Behaviour of disruption generated runaways in JET." Nuclear fusion, **42** (2002) 1039.

[12] O. N. Jarvis et al., "Photoneutron production accompanying plasma disruptions in JET." Nuclear fusion, **28** (1988) 1981.

[13] V. V. Plyusnin et al., "Study of runaway electron generation during major disruptions in JET." Nuclear Fusion, **46** (2006) 277.

[14] J. A. Wesson et al., "Disruptions in JET." Nuclear Fusion, **29** (1989) 641.

[15] C. Reux et al., "Runaway electron beam generation and mitigation during disruptions at JET-ILW." Nuclear Fusion, **55** (2015) 093013.

[16] R. Nygren et al., "Runaway electron damage to the Tore Supra Phase III outboard pump limiter." Journal of nuclear materials, **241** (1997) 522.

[17] A. H. Boozer, "Theory of runaway electrons in ITER: Equations, important parameters, and implications for mitigation." Physics of Plasmas, **22** (2015) 032504.

[18] M. Lehnen et al., "Disruptions in ITER and strategies for their control and

mitigation." Journal of Nuclear materials, **463** (2015) 39.

[19] E. M. Hollmann et al., "Status of research toward the ITER disruption mitigation system." Physics of Plasmas, **22** (2015) 021802.

[20] M. Lehnen et al., "Suppression of runaway electrons by resonant magnetic perturbations in TEXTOR disruptions." Physical review letters, **100** (2008) 255003.

[21] M. Gobbin et al., "Runaway electron mitigation by applied magnetic perturbations in RFX-mod tokamak plasmas." Nuclear Fusion, **57** (2016) 016014.

[22] S. Munaretto et al., "Effect of resonant magnetic perturbations on three dimensional equilibria in the Madison Symmetric Torus reversed-field pinch." Physics of Plasmas, **23** (2016) 056104.

[23] E. M. Hollmann et al., "Experiments in DIII-D toward achieving rapid shutdown with runaway electron suppression." Physics of Plasmas, **17** (2010) 056117.

[24] O. Ficker et al., "Runaway electron beam stability and decay in COMPASS." Nuclear Fusion, **59** (2019) 096036.

[25] D. Shiraki et al., "Dissipation of post-disruption runaway electron plateaus by shattered pellet injection in DIII-D." Nuclear Fusion, **58** (2018) 056006.

[26] M. R. Ghanbari et al., "Runaway electron generation decrease during a major disruption by limiter biasing in tokamaks." Radiation Effects and Defects in Solids, **168** (2013) 664.

[27] A. Alavi et al., "Prediction of hard x-ray behavior by using the NARX neural network to reduce the destructive effects of runaway electrons in tokamak." Physica Scripta, **96** (2021) 125625.

[28] Y. Liu, et al. "Toroidal modeling of runaway electron loss due to 3-D fields in DIII-D and COMPASS." Physics of Plasmas, **27** (2020) 102507.

[29] M. Landreman et al., "Numerical calculation of the runaway electron distribution function and associated synchrotron emission." Computer Physics Communications, **185** (2014) 847.

[30] K. Björk et al., "Kinetic modelling of runaway electron generation in argon-induced disruptions in ASDEX Upgrade." Journal of Plasma Physics, **86** (2020) 855860401.

[31] S. H. Saadat et al., "Stochastic modeling of plasma mode forecasting in tokamak." Journal of Plasma Physics, **78** (2012) 99.

[32] F. Matos et al., "Classification of tokamak plasma confinement states with convolutional recurrent neural networks." Nuclear Fusion, **60** (2020) 036022.

[33] R. M. Churchill et al., "Deep convolutional neural networks for multi-scale time-series classification and application to tokamak disruption prediction using raw, high temporal resolution diagnostic data." Physics of Plasmas, **27** (2020) 062510.

[34] W. Zheng et al., "Disruption predictor based on neural network and anomaly detection on J-TEXT." Plasma Physics and Controlled Fusion, **62** (2020) 045012.

[35] K. L. van de Plassche et al., "Fast modeling of turbulent transport in fusion plasmas using neural networks." Physics of Plasmas, **27** (2020) 022310.

[36] B. Yang et al., "Modeling of the HL-2A plasma vertical displacement control system based on deep learning and its controller design." Plasma Physics and Controlled Fusion, **62** (2020) 075004.

[37] N. Karayiannis, N.V. Anastasios. Artificial neural networks: learning algorithms, performance evaluation, and applications. Springer Science & Business Media, **209** (1992).

[38] A. N. James et al., "Measurements of hard x-ray emission from runaway electrons in DIII-D." Nuclear Fusion, **52** (2011) 013007.

[39] M. T. Hagan et al., "An introduction to the use of neural networks in control systems." International Journal of Robust and Nonlinear Control: IFAC-Affiliated Journal, **12** (2002) 959.

[40] K. Guo, "Research on location selection model of distribution network with constrained line constraints based on genetic algorithm." Neural Computing and Applications, **32** (2020) 1679.

[41] Wei Han, Hua Bao, and Xiulin Ruan, "Genetic algorithm-driven discovery of unexpected thermal conductivity enhancement by disorder." Nano Energy, 71 (2020) 104619.

[42] M. Jawad et al., "Genetic algorithm-based non-linear auto-regressive with exogenous inputs neural network short-term and medium-term uncertainty modelling and prediction for electrical load and wind speed." The Journal of Engineering, **2018** (2018) 721.

[43] L. Liu et al., "Optimizing an ANN model with genetic algorithm (GA) predicting load-settlement behaviours of eco-friendly raft-pile foundation (ERP) system." Engineering with Computers, **36** (2020) 421.

[44] Y. Zhou et al., "Hybrid genetic algorithm method for efficient and robust evaluation of remaining useful life of supercapacitors." Applied Energy, **260** (2020) 114169.

[45] H. Liang et al., "An improved genetic algorithm optimization fuzzy controller applied to the wellhead back pressure control system." Mechanical Systems and Signal Processing, **142** (2020) 106708.

[46] A. Al Mamun et al., "A comprehensive review of the load forecasting techniques using single and hybrid predictive models." IEEE Access, **8** (2020) 134911.

[47] M. Albadr et al., "Genetic algorithm based on natural selection theory for optimization problems." Symmetry, **12** (2020) 1758.

[48] Y. Sun et al., "Automatically designing CNN architectures using the genetic algorithm for image classification." IEEE transactions on cybernetics, **50** (2020) 3840.

[49] H. Dreicer, "Electron and ion runaway in a fully ionized gas. I." Physical Review, **115** (1959) 238.

[50] H. Dreicer, "Electron and ion runaway in a fully ionized gas. II." Physical review, **117** (1960) 329.

[51] Y. Sokolov, "Multiplication"of accelerated electrons in a tokamak." JETP Letters, **29** (1979).

[52] R. Jayakumar et al., "Collisional avalanche exponentiation of runaway electrons in electrified plasmas." Physics Letters A, **172** (1993) 447.

[53] M. N. Rosenbluth and S. V. Putvinski. "Theory for avalanche of runaway electrons in tokamaks." Nuclear fusion, **37** (1997) 1355.

[54] M. Gobbin et al., "Runaway electron mitigation by 3D fields in the ASDEX-Upgrade experiment." Plasma Physics and Controlled Fusion, **60** (2017) 014036.

[55] A. Lvovskiy et al., "The role of kinetic instabilities in formation of the runaway electron current after argon injection in DIII-D." Plasma Physics and Controlled Fusion, **60** (2018) 124003.

[56] V. V. Plyusnin et al., "Hard X-ray Bremsstrahlung of relativistic Runaway Electrons in JET." Journal of Instrumentation, **14** (2019) C09042.

[57] D. Graupe, Principles of artificial neural networks. World Scientific, 7 (2013).

[58] Z. Y. Chen et al., "Investigation of the effect of electron cyclotron heating on runaway generation in the KSTAR tokamak." Physics Letters A, **375** (2011) 2569.